Proceedings of the ASME 2010 3rd Joint US-European Fluids Engineering Summer Meeting and 8th International Conference on Nanochannels, Microchannels, and Minichannels
FEDSM-ICNMM2010
August 1-5, 2010, Montreal, Canada

FEDSM-ICNMM2010-31038

EXPERIMENTAL ANALYSIS OF NON-UNIFORM SURFACE ROUGHNESS AFFECTING TO FLOW RESISTANCE.

A. Matsumoto
Tokyo University of Science
Noda, Chiba, Japan

T. Ito
Tokyo University of Science
Noda, Chiba, Japan

M. Motozawa
Tokyo University of Science
Noda, Chiba, Japan

H. Kawashima
National Maritime Research Institute
Mitaka, Tokyo, Japan

H. Ando
National Maritime Research Institute
Mitaka, Tokyo. Japan

T. Senda
National Maritime Research Institute
Mitaka, Tokyo, Japan

Y. Kawaguchi
Tokyo University of Science
Noda, Chiba, Japan

ABSTRACT

Experimental investigation on non-uniform surface roughness affecting to flow resistance has been carried out. Experiment was performed with the concentric cylinder device. In this experiment, we evaluated non-uniform surface roughness of various surface by the optical method and measured friction coefficient in turbulent flow over each surface roughness. As an evaluation of non-uniform surface roughness, we measured surface roughness profiles of each surface by a laser displacement sensor. Based on this surface roughness profiles, we calculated some roughness parameters such as the root mean square roughness. One important result indicates the relationship between friction coefficient and roughness Reynolds number. The friction coefficient increases logarithmically with increasing roughness Reynolds number. Moreover, to discuss the effect of non-uniform roughness in detail, the Probability Density Function (PDF) of the roughness height and the spectrum of the surface roughness profiles were analyzed. As a result, the frictional drag over the rough surface can be mostly evaluated by the roughness Reynolds number which is defined by the root mean square roughness when the probability density distribution of the surface roughness profile has Gaussian distribution. However, if the probability density distribution does not have Gaussian distribution, kurtosis and skewness of surface roughness profile are also important parameter for the evaluation of the surface roughness.

NOMENCLATURE

C_f	Friction coefficient of test cylinders
C_{f0}	Friction coefficient of ST cylinder
C_f^*	Friction coefficient friction ratio between ST and test cylinders, (= C_f/ C_{f0})
$C_{f,fit}^*$	Friction coefficient ratio of fitted curve
E	Power spectrum
H	Roughness height, (m)
H^+	Roughness height normalized by frictional velocity
h	Height of inned cylinder, (0.3 m)
k_{ku}	Kurtosis of the surface roughness
k_s	Sand grain roughness
k_s^+	Roughness Reynolds number defined by k_s
k_{sk}	Skewness of the surface roughness
k_{rms}	Root mean square roughness
k_{rms}^+	Roughness Reynolds number defined by k_{rms}
k_x	Wave number of x direction
R_i	Radius of inner cylinder, (0.155 m)
R_o	Radius of outer cylinder, (0.165 m)
Re	Reynold number
T	Torque of shaft, (N·m)
u_τ	Frictional velocity, (m/s) $=\sqrt{\tau_w / \rho}$
δ	Half width between inner cylinder and outer cylinder, (0.005 m)
τ_w	Wall shear stress of inner cylinder, (Pa)

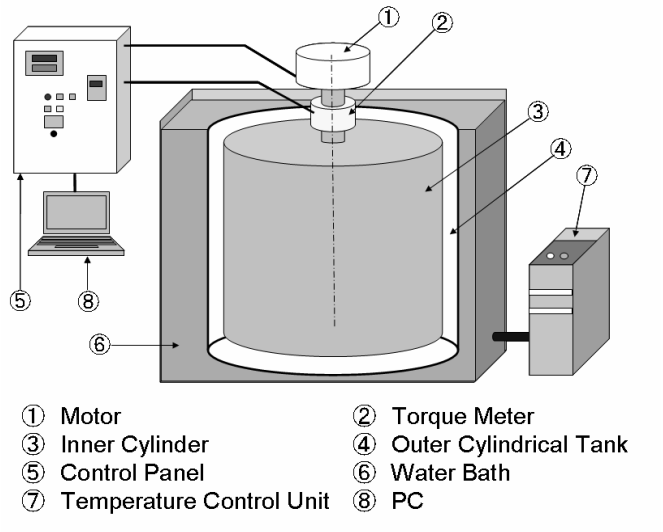

Fig. 1 Experimental Facility.

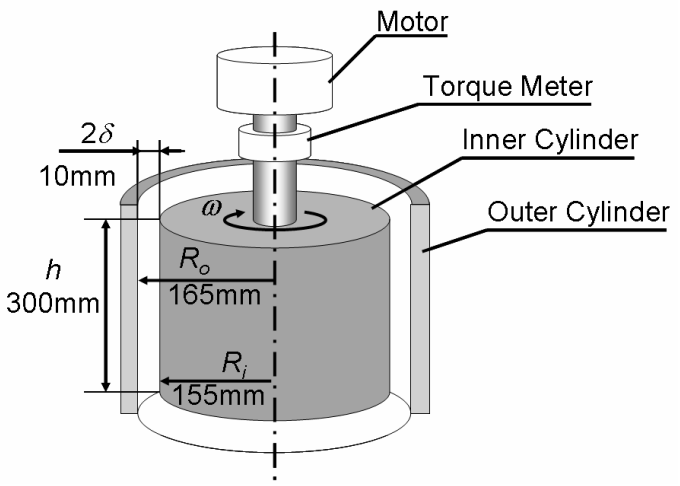

Fig. 2 Detailed Structure of the Test Section.

INTRODUCTION

Large amount of studies for turbulent flow over rough surface to clarify the relationship between frictional drag and surface roughness have been performed for a long time with great engineering interest because the engineering applications such as sailing ship hulls and industrial piping system involving turbulent flow over surface roughness. Particularly, pioneering work for the effect of surface roughness in pipe flow was carried out by Nikuradse[1], Colebrook and White[2].

Nikuradse investigated the effect of uniform sand roughness k_s on turbulent pipe flow by using various pipes which are internally roughened by a uniform layer of sand. He found that roughness Reynolds number (k_s^+) has close relationship with the frictional drag. The k_s^+ is defined as $k_s^+ = u_\tau k_s / \nu$. Here, u_τ and ν are frictional velocity and kinematic viscosity of water, respectively. In case of the pipes for $k_s^+ < 4$, friction coefficient changes with increasing Reynolds number. Therefore, such pipes have quite smooth surface. On the contrary, in case for $k_s^+ > 60$, friction coefficient becomes independent of Reynolds number and depends only on the roughness scale. Nikuradse defined this regime as fully roughness. Between these values for $4 < k_s^+ < 60$, flow behavior is in a transitional state in which both Reynolds numbers and grain size influence the frictional drag.

According to the definition by Nikuradse, roughness is often described in terms of characteristic roughness height. The characteristic height may be taken as the equivalent sand grain roughness height. This roughness is called as "uniform roughness". Several experimental studies[3,4] for the effect of uniform surface which is made up by sand grain, woven mesh and rod, on turbulent flow have been conducted. Especially, one of the most famous researches was conducted by Moody. Moody[5] guided largely by the finding of Colebrook, developed diagram to predict the head losses in smooth and rough pipe. The Moody diagram has been essential in the field of industry nowadays. In the recent study, Bergstrom *et al.*[6] investigated the effect of surface roughness on the velocity profile for three different types of the roughness elements; sand grains, wire mesh and perforated plate.

However, roughness encountered in nature is more complicated because the roughness height and pitch to height vary irregularly. This roughness encountered in nature can be called as "non-uniform roughness". Considering non-uniform roughness, because peak of roughness height and spatial frequency of surface roughness also have close relationship with flow resistance, it is necessary to evaluate the effect of surface roughness more precisely. Based on this background, there need to review classical Moody diagram by using novel technology in recent years. Actually, the effect of non-uniform roughness on the turbulent flow has been investigated by numerical simulation. Napoli *et al.* [7] carried out a numerical investigation of the flow over irregularly distributed two-dimensional roughness. In their study, the corrugated roughness is constructed by superposition of sinusoids of random amplitude. On the other hand, Bailon-Cuba *et al*. [8] performed the direct numerical simulation (DNS) for random height roughness effect on the turbulent channel flow and observed pressure distribution near the channel wall.

In this study, to investigate the effect of non-uniform roughness on flow resistance, we actually evaluated various surface roughnesses by the optical method and measured friction coefficient of each surface roughness in turbulent flow. In our experiment, surface roughness profiles of each surface roughness were measured by using a laser displacement sensor. Therefore, we can calculate some roughness parameters such as the root mean square roughness from this surface roughness profiles. Moreover, in order to more detailed investigation, the Probability Density Function (PDF) of the roughness height and the spectrum of the surface roughness profiles were analyzed. Based on these analyses for the non-uniform roughness, the effect of the non-uniform roughness on the flow resistance was discussed.

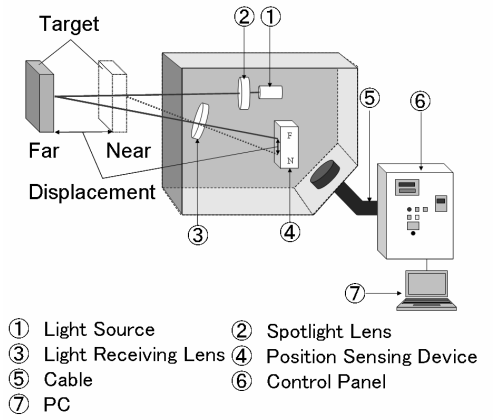

Fig. 3 Optics System of Laser Displacement Sensor.

EXPERIMENTAL METHOD

Experimental Apparatus

Figure 1 shows the schematic diagram of our experimental apparatus. The experiment was performed with the concentric cylinder device. The test section of this device is composed of outer cylindrical tank and inner cylinder (test cylinder). We prepared seven inner cylinders having various surface roughnesses. In the experiment, the outer cylindrical tank is filled with pure water and inner test cylinder sinks to the pure water. Then, the inner cylinder is rotated and the torque (T) of the shaft can be measured by the torque meter. Temperature of the water in outer cylindrical tank is stabled to constant by the temperature control unit which is composed of the water bath and the cooler.

The detailed structure of the test section is shown in Fig. 2. The radius of inner cylinder (R_i) is 0.155 m, and the radius of outer cylinder (R_o) is 0.165 m. The height of inner cylinder (h) is 0.3 m. Reynolds number based on the width between inner cylinder and outer cylinder (2δ) is defined as,

$$\mathrm{Re} = \frac{\omega R_i (R_o - R_i)}{\mu / \rho} = \frac{2\delta\omega R_i}{\mu / \rho} \tag{1}$$

where, ω is the angular velocity of the inner cylinder, μ and ρ are viscosity and density of pure water, respectively. This device allows wide range of Reynolds number from 60000 to 180000 with changing the rotational number (angular velocity).

The wall shear stress of the inner cylinder (τ_w) can be calculated by the torque of the inner cylinder as following equation,

$$\tau_w = \frac{T}{2\pi R_i^2 h} \tag{2}$$

The friction coefficient of the inner cylinder (C_f) is represented as,

$$C_f = \frac{\tau_w}{\frac{1}{2}\rho(\omega R_i / 2)^2} \tag{3}$$

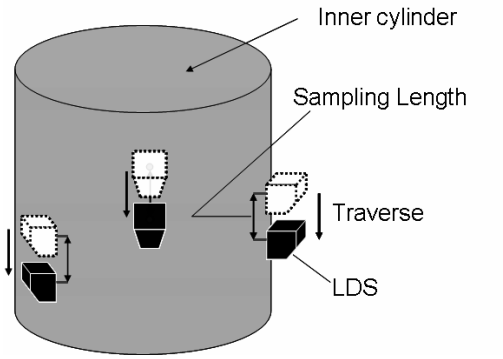

Fig. 4 Measuring Method for Surface Roughness.

Surface Roughness Measurement

Non-uniform surface roughness of each inner test cylinder was evaluated by using a laser displacement sensor (LDS). The optics system of this LDS is shown schematically in Fig. 3. Laser light having 650 nm of wavelength is generated by a light source which is composed of diode laser. The optical axis of laser source is collimated with a spotlight lends (cylindrical rod lens). Laser light spot is projected to the target through the spotlight lens and this laser light is reflected from the object. Then, reflected laser light is condensed onto a one-dimensional position sensing device through the light receiving lens. Therefore, surface roughness profile can be traced with moving this LDS. Measurement range of this LDS is 20 ± 1mm and the spatial resolution is 0.1 μm. The diameter of the beam spot on the target is 25 μm.

Figure 4 shows our measuring method for the surface roughness profiles of the inner test cylinders. We traced the surface roughness profiles at 100 locations chosen randomly for each test cylinders. Sampling length of the surface roughness profile is set to 50 mm. Based on measured surface roughness profile, we calculated some roughness parameters such as the root mean square roughness.

Quantitative Statistics of Surface Roughness

We calculated root mean square roughness (k_{rms}), roughness Reynolds number (k_{rms}^+), skewness of the surface roughness (k_{sk}) and kurtosis of the surface roughness (k_{ku}) of each test cylinder as a roughness parameter based on measured roughness profiles. Each parameter is defined as follows:

Root mean square roughness: The k_{rms} is the standard deviation of the height of surface and useful index of the surface roughness. k_{rms} is defined following equation,

$$k_{rms} = \sqrt{\frac{1}{L}\int_0^L H(x)^2 dx} \tag{4}$$

where, $H(x)$ is the roughness height and the average value of $H(x)$ is zero, L is sampling length of the surface roughness profile.

Table 1 Roughness Statistics of Each Test Cylinders

Test Cylinder	Type of surface	k_{rms} (μm)	k_{sk}	k_{ku}	k_{rms}^+
ST	Vinyl chloride (Standard)	0.8	0.02	3.52	0.25
SM 1	Waterborne acrylic plastic (Smooth 1)	5.7	0.00	3.18	1.67
SM 2	Waterborne acrylic plastic (Smooth 2)	14.2	0.32	3.96	4.17
TR 1	Marine paint (Transition 1)	26.6	1.62	9.05	8.93
TR 2	Waterborne acrylic plastic (Transition 2)	28.5	0.03	2.98	8.67
TR 3	Waterborne acrylic plastic (Transition 3)	27.8	0.11	3.56	8.38
RH	Sand grain (Fully Roughness)	161.7	-0.06	3.00	61.88

Roughness Reynolds number: The k_{rms}^+ is used to correlate the surface roughness to the flow behavior. This parameter is defined with k_{rms} and given by,

$$k_{rms}^{+} = \frac{k_{rms} u_\tau}{\nu} \tag{5}$$

where, u_τ is the friction velocity, ν is the kinematic viscosity of the fluid.

Skewness of surface roughness: The k_{sk} is the skewness of surface roughness. The skewness indicates the degree of symmetry of probability density function distribution. In negative or positive skewness, probability density function distribution is concentrated on the top or bottom and the bottom tail or top tail is longer. The k_{sk} is expressed as follows,

$$k_{sk} = \frac{1}{k_{rms}^{3}} \left[\frac{1}{L} \int_0^L H(x)^3 dx \right] \tag{6}$$

Kurtosis of surface roughness: The k_{ku} is the kurtosis of surface roughness. The kurtosis indicates the degree of sharp or blunt of surface roughness. The k_{ku} is given by

$$k_{ku} = \frac{1}{k_{rms}^{4}} \left[\frac{1}{L} \int_0^L H(x)^4 dx \right] \tag{7}$$

Test Cylinders

We prepared seven test inner cylinders. One test cylinder which is made of vinyl chloride has quite smooth surface. We named this test cylinder "ST (Standard)" in this paper. On the contrary, other six test cylinders have various rough surfaces. These surface roughnesses are made up with painting waterborne acrylic plastic, marine paint and sand on the surface of the standard cylinder. We classified these cylinders into "SM (Smooth)", "TR (Transition)" and "RH (Rough)" on the basis for the classification according to the roughness Reynolds number given by Nikuradse.

Table 1 lists root mean square roughness k_{rms}, roughness Reynolds number k_{rms}^+, skewness of the surface roughness k_{sk} and kurtosis of the surface roughness k_{ku} of each test cylinder. In addition, the surface roughness profiles of each test cylinders are shown in Fig. 5. x^* is defined as the sampling position x normalized by width between inner cylinder and outer cylinder (2δ=10 mm) and H^+ is defined as the roughness height (H) normalized by ν/u_τ. In this figure, u_τ is calculated under the experiment for Re = 91000. Detailed discussion for the surface roughness is given in next section.

RESULTS AND DISCUSSION

Surface Roughness

Table 1 and Fig. 5 show the roughness parameters and surface roughness profiles of each test cylinders, respectively. As shown in Table 1, the surface roughness of each test cylinders is divided into three groups (i.e. SM, TR and RH) based on the root mean square roughness k_{rms}. In this study, we defined roughness Reynolds number k_{rms}^+ which is defined with using the root mean square roughness k_{rms}.

It can be seen that the ST has quite smooth surface. There is no remarkable major peak through the surface profile of ST and ST has the lowest value of the root mean roughness k_{rms} of all test cylinders. Therefore, we defined this cylinder as the standard cylinder for the comparison with other test cylinders.

All of the cylinders except for TR 1 have almost 0 of the skewness of the surface roughness k_{sk} and about 3 of the kurtosis of the surface roughness k_{ku}. Therefore, the surface profiles of these surfaces have a nearly Gaussian probability density distribution and the roughness of these cylinders is geometrically similar.

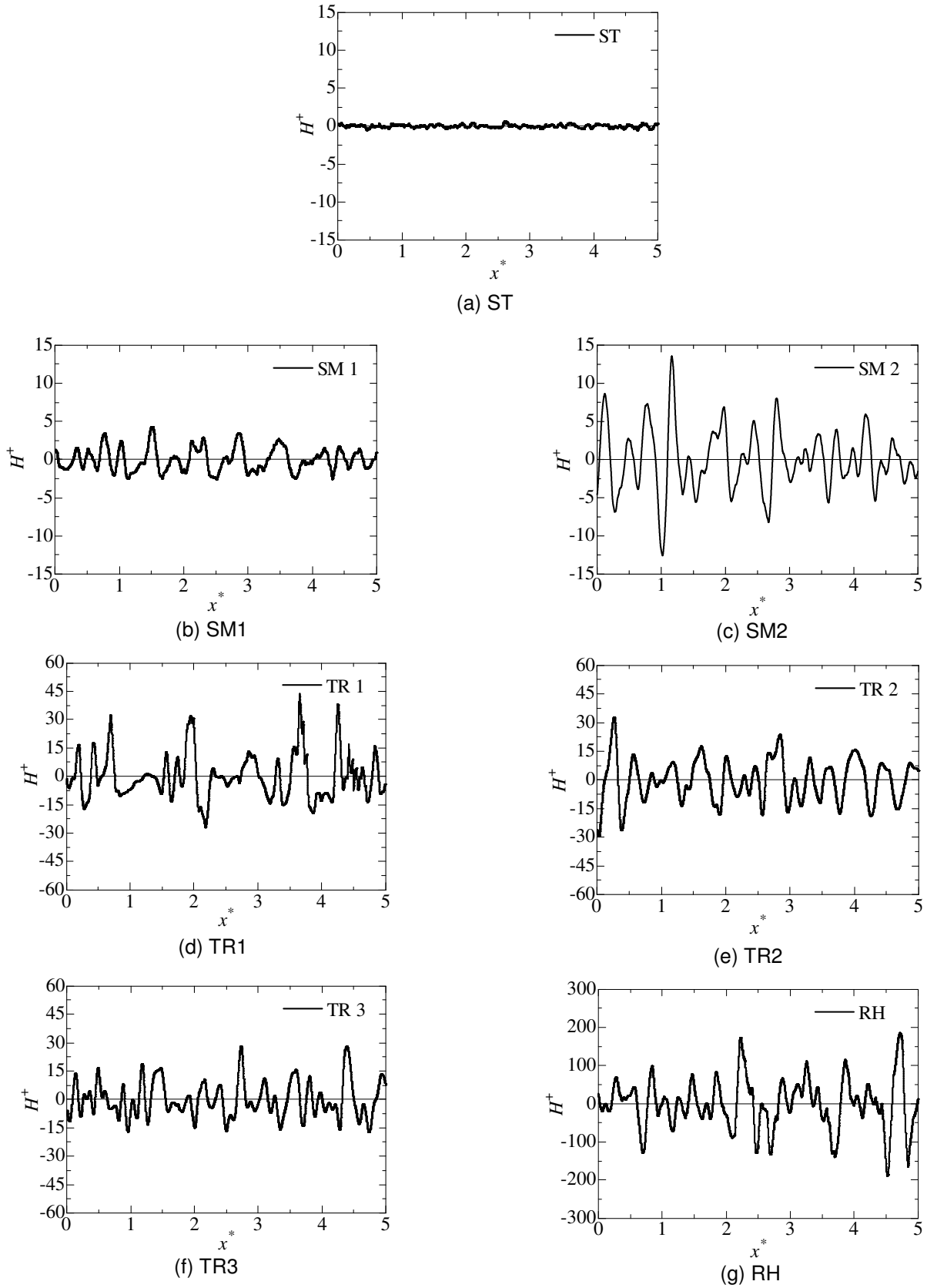

(a) ST

(b) SM1

(c) SM2

(d) TR1

(e) TR2

(f) TR3

(g) RH

Fig. 5 Surface Roughness Profiles for (a) ST, (b) SM1, (c) SM2, (d) TR1, (e) TR2, (f) TR3, (g) RH.

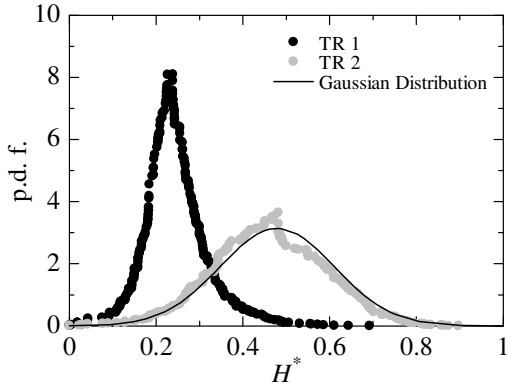

Fig. 6 Probability Density Distribution of Surface Profiles for TR 1 and TR 2.

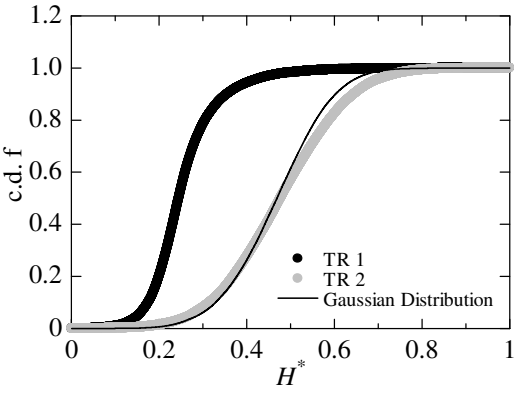

Fig. 7 Cumulative Density Distribution of Surface Profiles for TR 1 and TR 2.

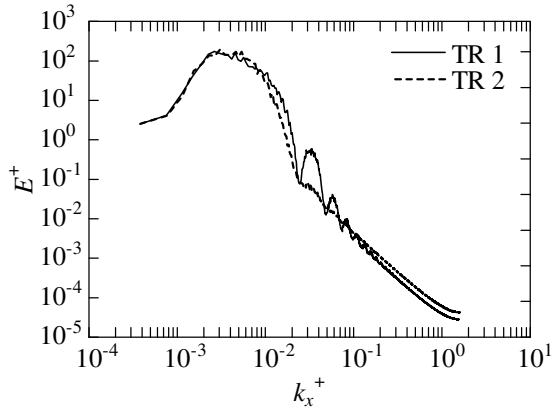

Fig. 8 Spectrum Analyses of Surface Profiles for TR 1 and TR 2

On the other hand, in case of the transitional roughness regime (i.e. TR 1, TR 2 and TR 3), though the root mean square roughness k_{rms} of TR 1, TR 2 and TR 3 have almost same value, the skewness of surface roughness k_{sk} and the kurtosis of surface roughness k_{ku} of TR 1 are quit different from TR 2 and TR 3. This indicates that TR 1 has geometrically different surface comparing with other cylinders. This geometrical difference in

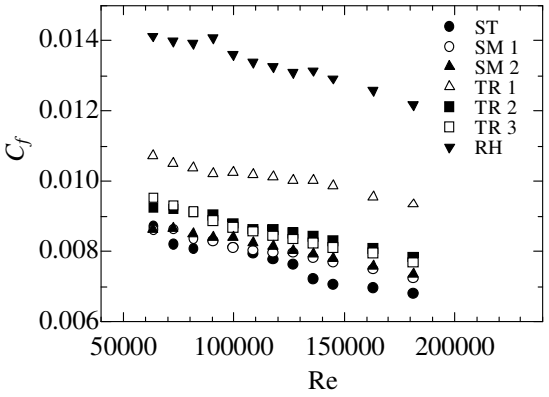

Fig. 9 Reynolds Number Dependence of Friction Coefficient.

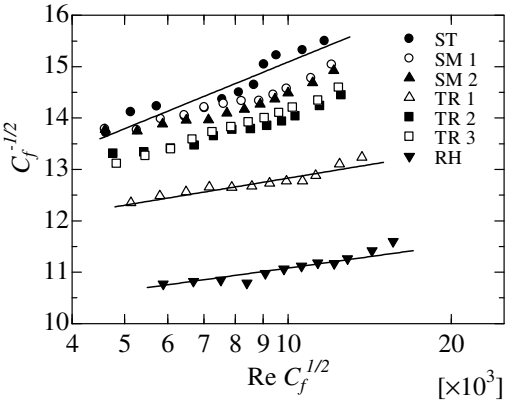

Fig. 10 Evaluation of Reynolds Number Dependence of Friction Coefficient proposed by Prandtl[11].

TR 1 seems to be derived by the characteristics of the roughness height and pitch to height of the surface profile. Comparing among Figs. 5(d), (e) and (f), the normalized roughness height of TR 1 is larger than that of TR 2 and TR 3 and the pitch to height of TR1 varies randomly.

Figures 6 and 7 show probability density distribution and cumulative density distribution of the roughness profiles for TR1 and TR2, respectively. Probability density distribution and cumulative density distribution of TR 2 show nearly Gaussian roughness distributions with a skewness of 0.03 and kurtosis of 2.98. It can be seen that the probability density function of TR1 is quite different from TR 2 though the root mean square roughness k_{rms} is almost same.

Figure 8 shows the result of the spectrum analysis of the surface roughness profile of TR1 and TR 2. E^+ is defined by $E/k_{rms}^2 (u_\tau/\nu)$, where E is power spectrum of surface roughness. Normalized power spectrum of TR 1 has almost same value with that of TR 2. This indicates that non-uniform surface roughness can be mostly evaluated by using root mean square roughness k_{rms}. However, this configuration of TR 1 is quite different from TR 2. It seems that surface of TR 2 has wavy wall geometry and TR 1 has spiny wall geometry. In addition, spectrum of TR 3 has almost same configuration with TR 2.

Table 2 Value of the Coefficient for Equation (8).

Test	C_1	C_2
ST	4.31	-2.15
SM 1	2.84	3.25
SM 2	2.69	3.73
TR 1	1.75	5.83
TR 2	2.68	3.29
TR 3	3.21	1.31
RH	1.47	5.20

Effect of Surface Roughness on Friction Coefficient

Figure 9 shows the friction coefficient for each test cylinders with variety of Reynolds number. This figure indicates that the friction coefficient increases with increasing surface roughness. The smallest friction coefficient is obtained for ST which has quite smooth surface. On the contrary, because RH has fully rough surface, the friction coefficient of RH is much lager than that of other cylinders.

In case of the transitional roughness regime (i.e. TR 1, TR2 and TR 3), characteristic result was obtained. The friction coefficient of TR 1 has about 20 % lager value than that of TR2 and TR 3. This indicates that the frictional drag of the turbulent flow over the rough surface can not be evaluated by only the root mean square roughness k_{rms} because the k_{rms} is almost same value for TR 1, TR 2 and TR 3. On the contrary, because TR 2 and TR 3 have similar geometrical surface (i.e. k_{rms}, k_{sk} and k_{ku} of TR 2 and TR3 have almost same value), almost same friction coefficient was obtained. As mentioned above, skewness of surface k_{sk} and kurtosis of the surface k_{ku} of TR 1 are quite different from TR 2 and TR 3. Therefore, k_{sk} and k_{ku} are also important parameters for evaluation of the relationship between the surface roughness and frictional drag in turbulent flow.

Schultz et al.[4] investigated the effect of surface roughness affected the slope of roughness shape. They prepared various rough surface consisted of close-packed pyramids and examined the effect of surface roughness with changing the pyramid heights and slope angle of the lateral edge. For high Reynolds number, the slope of the roughness is important parameter in the prediction of drag for roughness with shallow angles. In the surface with small slope, normalized mean velocity profile by the roughness function does not scale on the roughness height. This indicates that there are also correlations between the friction coefficient and spatial frequency of surface roughness. Moreover, Napoli *et al.* [7] carried out a numerical simulation of the flow over the irregular shape roughness with randomly distributed elements having different height. They developed a roughness parameter termed the effective slope, defined by ratio performed integration between roughness amplitude and stream wise direction. The effect of roughness increases with increased the effective slope. There may be correlations between this parameter and spatial frequency.

Therefore, not only k_{sk} and k_{ku} but also spatial frequency seems to be also important parameters for evaluation of the effect of the surface roughness on the flow resistance. However, it is difficult to discuss the effect of surface roughness with separating influence of k_{sk} and k_{ku} into influence of the spatial frequency by only one characteristic case for TR 1. Further detailed experiment is needed to understand the turbulent flow over the rough surface in the future.

Reynolds Number Dependence of Friction Coefficient

As shown in Fig. 9, the friction coefficient depends on Reynolds number for all cylinders. According to Nikuradse[1], Reynolds number dependence must be lost in the fully rough regime $k_s^+ > 60$. However, the friction coefficient of RH also depends on Reynolds number.

To investigate Reynolds number dependence of the friction coefficient in detail, the following relationship between friction coefficient and Reynolds number proposed by Prandtl[9]. This relation can be derived from integration of the mean velocity profile and given by,

$$\frac{1}{\sqrt{C_f}} = C_1 \log(\mathrm{Re}\sqrt{C_f}) + C_2 \tag{8}$$

where, C_1 and C_2 are coefficients and the value of C_1 directly indicated the strength of the Reynolds number dependence. Therefore, as the friction coefficient becomes independent of Reynolds number for fully rough surface or large Reynolds number, coefficient C_1 approaches 0.

Figure 10 shows the relation between $C_f^{-1/2}$ and $\mathrm{Re}\cdot C_f^{1/2}$ for each cylinders and Table 2 displays the value of coefficient C_1 and C_2 obtained by this experiment. The coefficient C_1 for ST has largest value of all cylinders. This indicates that Reynolds number dependence on the friction coefficient is much stronger relatively than that of other cylinders because the surface of ST is rather smooth.

As mentioned above, in pipe flow, the friction coefficient must be independent of Reynolds number in the fully rough regime for $k_s^+ > 60$ in the same range of Reynolds number with our experiment. However, in this experiment, though RH has fully rough surface, the friction coefficient of RH also has Reynolds number dependence with $C_1 = 1.47$. This is because the experimental system is different. Nikuradse used the pipe which is internally roughned by a uniform layer of sand. The test pipe diameter ranged from 8 to 21 mm. On the contrary, we used the concentric cylinder device which has rough surface of inner cylinder and smooth surface of outer cylinder tank having 10 mm of the width between inner cylinder and outer cylinder.

Berg *et al.* [10] examined the torque required to drive the smooth or rough cylinders in turbulent Taylor-Couette flow. The experimental apparatus consists of rotating inner cylinder with 0.16 m of radius and outer cylinder with 0.22 m of radius. They investigated with changing the surface roughness of the inner cylinder and outer cylinder. In their experiment which was

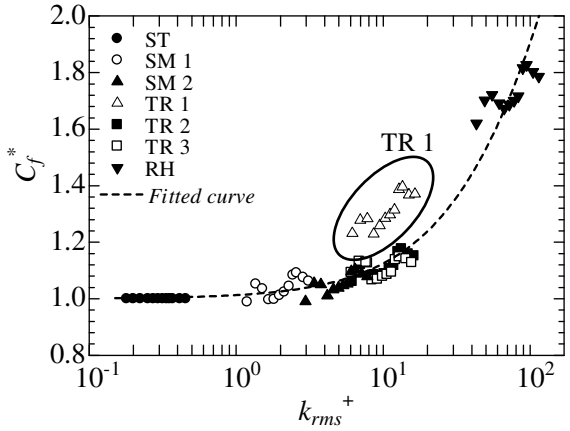

Fig. 11 Roughness Reynolds Number k_{rms}^+ Dependence of the Friction Coefficient Ratio.

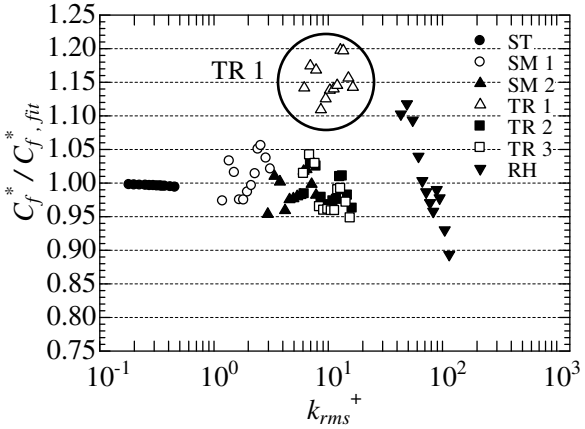

Fig. 12 Comparison of the Friction Coefficient Ratio between Experiment Results and Fitted Curve for Fig.10.

performed between rough surface of inner cylinder and smooth surface of outer cylinder in the same condition with our experiment for RH, the friction coefficient also depends on Reynolds number in the same range of Reynolds number with our experiment. Therefore, similar tendency of Reynolds number dependence in fully rough regime seems to be obtained in the concentric cylinder device in our experiment.

Finally, in case of the transitional regime, coefficient C_1 of TR 1 has smaller value than that of TR 2 and TR 3 and almost same with RH. This indicates that Reynolds number dependence of TR 1 is smaller relatively same as the fully roughness regime RH. The roughness profile of TR 1 has larger roughness height and lower spatial frequency of the roughness peak than that of TR 2 and TR 3. This roughness height of TR 1 reaches the fully roughness regime. As a result, though the root mean square roughness k_{rms} of TR 1 is much smaller than that of RH, similar Reynolds number dependence with RH was obtained in TR 1. In addition, because the surface roughness of TR 2 and TR 3 is geometrically similar, C_1 of TR 2 and TR 3 have almost same value.

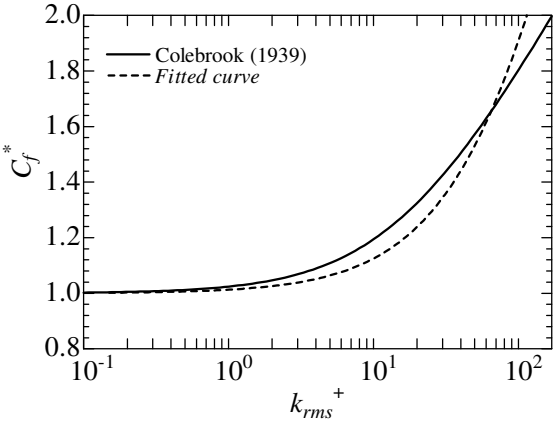

Fig. 13 Comparison of Surface Roughness Influence between Non-Uniform Roughness (our Experiment) and Uniform Roughness (Colebrook's Result).

Roughness Reynolds Number Dependence of the Flow Resistance

Figure 11 shows the roughness Reynolds number dependence of the flow resistance. In this figure, the friction coefficient ratio C_f^* is defined as C_f / C_{f0}. Here, C_{f0} and C_f is the friction coefficient of ST and each cylinder, respectively. This figure indicates that the friction coefficient ratio has close relationship with the roughness Reynolds number defined with the root mean roughness k_{rms}. The friction coefficient ratio increases logarithmically with increasing roughness Reynolds number.

The broken line named "fitted curve" in this figure represents following equation,

$$C_{f,fit}^* = 1 + \frac{1.27}{0.421}\log(1 + 0.01 k_{rms}^+) \qquad (9)$$

Figure 12 shows the results of the comparison between the experimental results and fitted curve for all cylinders. Fitted curve was decided with the dispersion of $C_f^* / C_{f,fit}^*$ to have the smallest value except for the experimental results of TR 1. As shown in Figs. 11 and 12, experimental results for all cylinders except for TR 1 have good agreement with the fitted curve and $C_f^* / C_{f,fit}^*$ stays within only ±0.05 except for TR 1 and RH. This indicates that the frictional drag over the rough surface can be mostly evaluated by the roughness Reynolds number k_{rms}^+ which is defined by the root mean square roughness k_{rms} when the probability density distribution of the surface roughness profile has Gaussian distribution.

Comparison with Colebrook's Result

Figure 13 shows the comparison of the roughness Reynolds number dependence of the friction coefficient between fitted curve obtained by our experiment (non-uniform roughness) as shown in Fig. 10 and Colebrook's result[2] (uniform roughness). Colebrook *et al*. investigated the effect of uniform

sand roughness k_s on turbulent pipe flow by using various pipes which are internally roughened by a uniform layer of sand. They obtained the relation among uniform sand surface roughness, friction coefficient of pipe and Reynolds number with following equation,

$$\frac{1}{\sqrt{\lambda}} = -2.0\left(\frac{k_s}{d} + \frac{9.34}{\mathrm{Re}\sqrt{\lambda}}\right) + 1.14 \qquad (10)$$

To compare with our experiment, the pipe diameter d is given 10 mm same as the width between the inner cylinder and outer cylinder and the equivalent sand grain roughness k_s is taken to be $3.0k_{rms}$. This relationship between k_s and k_{rms} was referred by Zagarola and Smits [11].

As a result of this comparison, the fitted curve obtained by our experiment satisfactorily agrees well with the Colebrook's result. This indicates that non-uniform surface roughness has almost same effect on the turbulent flow with the uniform surface roughness under the limited condition that the surface roughness profile has the Gaussian distribution. Moreover, under this limited condition, we can use the root mean roughness as an index of the roughness parameter.

CONCLUSION

Effect of the non-uniform rough surface on the flow resistance was investigated experimentally. Experiment has been performed with the concentric cylinder device. We prepared seven test cylinders having various surface roughnesses and classified into ST, SM. TR and RH for the basis of the effect of the surface roughness on the frictional drag classified by the Nikuradse. Non-uniform surface roughness of each cylinder was evaluated by the laser displacement sensor and friction coefficient in turbulent flow over each surface roughness was measured with changing wide range of Reynolds number. The main conclusions are drawn as follows.

1. The frictional drag over the rough surface can be mostly evaluated by the roughness Reynolds number which is defined by the root mean square roughness k_{rms} if the probability density function of the surface roughness has Gaussian distributions. The friction coefficient increases logarithmically with increasing roughness Reynolds number.
2. Though the root mean square roughness k_{rms} of TR 1, TR 2 and TR 3 have almost same value, the skewness of surface roughness k_{sk} and the kurtosis of surface roughness k_{ku} of TR1 are quit different from TR 2 and TR 3. The probability density distributions of roughness profile of TR 2 and TR 3 have Gaussian distribution. The friction coefficient of TR 2 and TR 3 has almost same value, but the friction coefficient of TR 1 has about 20 % lager value than that of TR2 and TR3. Therefore, the frictional drag of the turbulent flow over the rough surface can not be evaluated by only the root mean square roughness k_{rms}.
3. The fitted curve of the relation between the friction coefficient and roughness Reynolds number obtained by our experiment (non-uniform roughness) has good agreement with the Colebrook's result (uniform roughness).

ACKNOWLEDGMENTS

This study has been supported by New Energy and Industrial Technology Development Organization (NEDO). We would like to thank Mr. T. Ashida of the Chugoku Marine Paint, Ltd., Dr. K.Iwamoto of the Tokyo University of Agriculture and Technology and Mr. S. Ishitsuka and Mr. T. Kurosawa of the Tokyo University of Science for the supporting in this study.

REFERENCES

[1] J. Nikrase, Strömungsgesetze in Rauhen Rohren, *VDI-Forsch.*, 361(1933). (Eng. Transl; Laws of flow in tough pipes, *NAKA TM*, 1292)

[2] C. F. Colebrook and C. M. White, Experiments with Fluid Friction in Roughned Pipes, *Proc. R. Soc. Lond A*. 161(1937), pp. 367-381.

[3] P. A. Krogstad and R. A. Antonia, Surface Roughness Effects in Turbulent Boundary Layers, *Exp. Fluids*, 27(1999), pp. 450-460.

[4] M. P. Schultz and K. A. Flack, Turbulent Boundary Layers on a Systematically Varied Rough Wall, *Phys. Fluids*, 21(2009), 015104.

[5] L. F. Moody, Friction Factors for Pipe Flow, *Trans. ASME*, 66(1944), pp. 671-684.

[6] D. J. Bergstrom, N. A. Kotey and M. F. Tachie, The Effects of Surface Roughness on the Mean Velocity Profile in a Turbulent Boundary Layer, *Trans. ASME*, 124(2002), pp. 664-670.

[7] E. Napoli, V. Armenio and M. De Marchis, The Effect of the Slope of Irregularly Distributed Roughness Elements on Turbulent Wall-Bounded Flows, *J. Fluid Mech.* 613(2008), pp. 385-394.

[8] J. Bailon-Cuba, S. Leonardi and L. Castillo, Turbulent Channel Flow with 2D Wedges of Random Height on One Wall, *J. Heat Fluid Flow*, 30(2009), pp. 1007-1015.

[9] L. Prandtl, Neuere Ergebnisse der Turbulentzforschung, *Zeitschrift des Vereines deutscher Ingenieure*, 7(1933), pp. 105-114. (Eng. Tansl; Recent Results of Turbulence Research, *NACA TM*, 720)

[10] T. H. van den Berg, C. R. Doering, D. Lohse and D. P. Lathrop, Smooth and Rough Boundaries in Turbulent Taylor-Couette Flow, *Phy. Rev. E,* 68(2003), 036307.

[11] M. V. Zagarola and A. J. Smits, Mean-Flow Scaling of Turbulent Pipe Flow, *J. Fluid Mech*. 373(1998), pp. 33-79.